

**MICROSTRUCTURAL STABILITY OF FULLY LAMELLAR Ti-45Al-5Nb-0.2B-0.75C ALLOY**

ČEGAN Tomáš, ŠPALEK František, ZIENTEK Stanislav, VONTOROVÁ Jiřina, STRUNG Václav

*VSB - Technical University of Ostrava, Ostrava, Czech Republic, Regional Materials Science and Technology Centre, Ostrava, Czech Republic, EU, [tomas.cegan@vsb.cz](mailto:tomas.cegan@vsb.cz)***Abstract**

The microstructural stability of fully lamellar  $\gamma$ -TiAl alloy was studied under thermal exposure at 750, 850 and 950 °C for 3400 h. The microstructure analysis shows that the most dominant change in the microstructure was that the  $\alpha_2$  lamellae thinned gradually and thinning was more pronounced with increasing temperature and with increasing time. Formation of recrystallized  $\gamma$  grains and  $Ti_2AlC$  carbides were also observed especially during the temperature 850 and 950 °C after prolonged heat treatment. The effect of microstructural changes during the thermal exposure on mechanical properties was evaluated and discussed.

**Keywords:** Titanium aluminides, thermal stability, microstructure, carbides

**1. INTRODUCTION**

Titanium aluminides based on  $\gamma$ -TiAl have been implemented for application as turbine blades and turbocharger wheels in high-performance combustion engines due to their low density combined with enhanced high-temperature strength and creep resistivity up to 750 °C as well as their good oxidation behavior [1]. Depending on the alloy composition and processing parameters, various microstructures can be obtained in this group of alloys. It is now well-established that  $\gamma$ -TiAl alloys with a fully lamellar microstructure have far superior creep properties than duplex and near- $\gamma$  microstructures [2]. However, their creep resistance at higher temperatures (above 800 °C) does not fulfil requirements of designers which hinders their some perspective applications. One of the possibilities to increase the resistance at these temperatures is alloying with higher amounts of heavy metals (W, Mo, Ta, Nb), which are characterized by high temperature resistance and in  $\gamma$ -TiAl alloys cause solid solution hardening [3-6]. A further step to improve the high temperature capability of advanced intermetallic  $\gamma$ -TiAl based alloys is alloying with carbon. Thereby, C can act as an efficient solid solution strengthener or form needle-shaped precipitates in the  $\gamma$ -phase [7, 8]. In spite of the previous studies which dealt with precipitation of carbides in  $\gamma$ -TiAl alloys [7-10], information about microstructural stability of carbon added alloys at higher temperatures and longer times is still lacking in the literature. Therefore, the aim of this article is to study long-term microstructural stability of the Ti-45Al-5Nb-0.2B-0.75C (at.%) alloy and effect of microstructural changes on mechanical properties during long-term ageing at temperatures 750, 850 and 950 °C was evaluated and discussed.

**2. EXPERIMENT**

The selected alloy was produced with using of a medium frequency vacuum induction melting furnace Supercast-titan. As charge were used pure metals (4N) and Nb-Al master alloy, which preparation, chemical composition and melting temperature were described elsewhere [11]. The as-cast cylindrical bars with a diameter of 20 mm and length of 225 mm were subjected to a hot isostatic pressing (HIP) at an applied pressure of 180 MPa and temperature of 1270 °C for 4 h in order to eliminate casting porosity. A fully lamellar  $\gamma(TiAl)/\alpha_2(Ti_3Al)$  microstructure of the bar was produced by heat treatment consisting of solution annealing and cooling to room temperature. The solid solution annealing was performed in a single  $\alpha$  phase (Ti-based solid solution with hexagonal crystal structure) field at 1360 °C for 1 h followed by cooling at a constant cooling rate of 20 °C/min to 850 °C under argon atmosphere. The heat treatment was accomplished by the cooling to room

temperature in air. After the heat treatment, the bar was cut by electro spark machining into small pieces with a diameter of 20 mm and length of 12 mm. The ageing experiments were performed at three temperatures of 750, 850 and 950 °C up to 3400 h in resistance tube furnaces with static argon atmosphere. The samples were observed by optical microscopy on the microscope Olympus GX51 equipped with digital camera Olympus DP12 (OM), scanning electron microscopy in the mode of back-scattered electrons (BSEM) using microscopes QUANTA FEG 450 and JSM-7600F equipped with an energy dispersive spectrometer (EDS) and by X-ray diffraction (XRD). Transmission electron microscopy (TEM) was performed by JEM-2100 microscope operating at 200 kV. Samples for TEM with an initial thickness of 0.3 mm were thinned mechanically by grinding to a thickness of 100 µm and finally thinned electrolytically in electrolyte A3 Struers with using TenuPol-3 device operating at a voltage of 20 V and solution temperature of -20 °C. Oxygen and carbon contents were measured by thermo-evolution method by analysers ELTRA ONH-2000 and ELTRA CS-2000, respectively. Quantitative metallographic analysis was performed on digitalized micrographs using a computerized image analyser SigmaScanPro. For determination of the average lamellar thickness and for the determination of the distribution of lamellae thickness at least 1000 individual lamellae in at least 20 different grains were measured for each sample. For determination of the  $\alpha_2$  phase content at least 20 digitalized images were measured. Vickers microhardness measurements were performed at a constant load of 1 N for loading time of 10 s on polished and slightly etched samples.

**Table 1** Nominal and measured chemical composition of the alloy (at.%)

	Ti	Nb	Al	B	C	O
Nominal	Bal.	5	45	0.2	0.75	-
Measured	Bal.	5.21 ± 0.10	45.33 ± 1.13	-	0.69 ± 0.01	0.13 ± 0.02

### 3. RESULTS

#### 3.1. Microstructure before thermal exposure

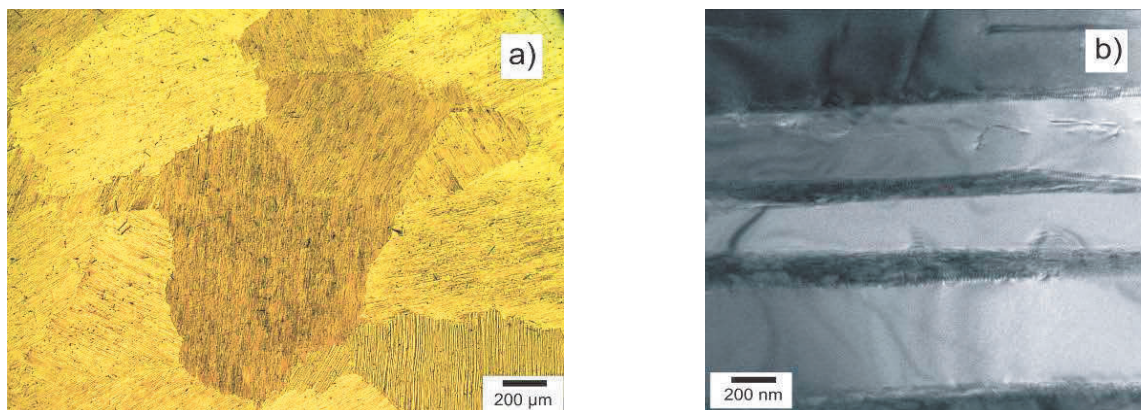


**Figure 1** (a) Microstructure before thermal exposure (OM) (b) Bright field image of microstructure before thermal exposure (TEM)

The measured chemical composition of the as-cast alloy is very close to the nominal composition, as seen in **Table 1**. The oxygen content of 0.13 at.% (490 wt.ppm) meets the requirements for the industrial applications where the maximum allowable oxygen content is usually reported to be about 500 wt. ppm [12]. **Figure 1(a)** shows the microstructure of the alloy after solid solution annealing followed by the cooling at a constant cooling rate of 20 °C/min to 850 °C and free air cooling to room temperature. The microstructure consists of equiaxed grains with an average size of 385 µm. The microstructure of the grains is fully lamellar with average width of the  $\alpha_2$  and  $\gamma$  lamellae of (0.31 ± 0.04) and (0.42 ± 0.04) µm, respectively. The small bright particles in

**Figure 2(a)** are identified as (Ti,Nb)B borides, which is in agreement with the observations of similar type of alloys [13]. Quantitative metallographic analysis revealed that the lamellar grains contain about 37 vol. % of the  $\alpha_2$  phase and 63 vol.% of the  $\gamma$  phase. These results are in a good agreement with the results reported by Schwaighofer [7] for the TNM alloy with 0.75 at.% C. Relatively high volume fraction of the  $\alpha_2$  phase can be explained by a stabilizing effect of carbon [7, 8]. **Figure 1(b)** shows TEM bright field image of alloy after the heat treatment. In this figure, the lamellae contain no carbides, which clearly indicate that carbon remained completely dissolved in the  $\gamma$  and  $\alpha_2$  phases after the applied heat treatment. The absence of carbides was also confirmed by the results of X-ray diffraction (not shown in this article).

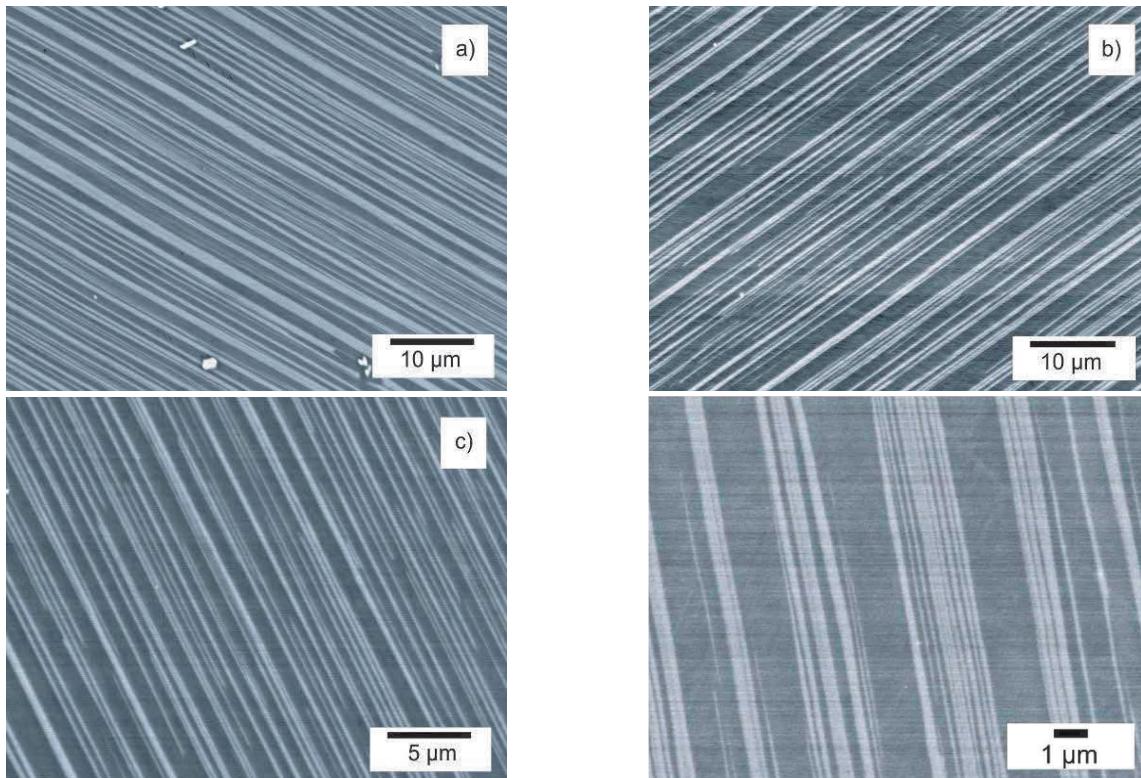


**Figure 2** SEM BSE images of lamellar structure after exposure at (a) 0 h (b) 950 °C, 2000 h (c) 750 °C, 3400 h (d) 850 °C, 960 h

### 3.2. The microstructure after thermal exposure

**Figure 2 (b-c)** shows the lamellar microstructure after exposure at 950 °C for 2000 h and 750 °C for 3400 h, respectively. In comparison with **Figure 2(a)** can be observed, that the dominant change in the lamellar grains was that the  $\alpha_2$  lamellae thinned gradually and become discontinuous. No decomposition of  $\alpha_2$  lamellae into  $\alpha_2$  +  $\beta$  and no recrystallization of  $\beta$  phase were observed. Only in some thick  $\alpha_2$  lamellas decomposition into refine  $\alpha_2$  +  $\gamma$  lamellae were detected (see **Figure 2(d)**). **Figure 3** shows the comparison of  $\alpha_2$  lamellae distribution in the sample before exposure and after 3400 h at 750, 850 and 950 °C. The results confirms the  $\alpha_2$  loss during ageing, because the frequency of thin lamellae  $\alpha_2$  are usually much higher in the samples after exposure at 850 and 950 °C than in the samples after exposure at 750 °C or before exposure. This phenomenon was also confirmed by the results of the average  $\alpha_2$  lamellae width measurements, which are 0.31, 0.26, 0.24 and 0.22  $\mu\text{m}$  for the sample before exposure and after exposure at 750, 850 and 950 °C for 3400 h, respectively. **Figure 4** shows the comparison of  $\gamma$  lamellae distribution in the sample before exposure and after 3400 h at 750, 850 and 950 °C. The results show that the width of  $\gamma$  lamellae increased during ageing, because the frequency of thin  $\gamma$  lamellae are usually much higher in the samples before exposure and after exposure at

750 °C, than after exposure at 850, or 950 °C for 3400 h and the samples after exposure at 850, or 950 °C for 3400 h showed a higher frequency of occurrence of coarse  $\gamma$  lamellae. This phenomenon also confirms the results of the average  $\gamma$  lamellae width measurements, which are 0.42, 0.46, 0.49 and 0.62  $\mu\text{m}$  for the sample before exposure and after exposures at 750, 850 and 950 °C for 3400 h, respectively. The  $\alpha_2$  loss during ageing is also apparent from the results of measuring of the  $\alpha_2$  phase content. The volume fraction of  $\alpha_2$  drops from 37 vol. % to 32, 29 and 23 vol. % for the sample before exposure and after exposures at 750, 850 and 950 °C for 3400 h, respectively. The drop in  $\alpha_2$  phase content is, however, much lower than were reported by Karthikeyan and Mills [14], whose reported a decrease of  $\alpha_2$  content in K5 and K5SC alloy from 22 and 29 vol. % before exposure to 8 and 7.2 vol.% after exposure at 900 °C for 24 h, respectively. This lower drop in the  $\alpha_2$  phase content may be associated with a higher C content in our alloy. Carbon is namely known as a distinctive alpha stabilizer and slows the decomposition of the  $\alpha_2$  phase.

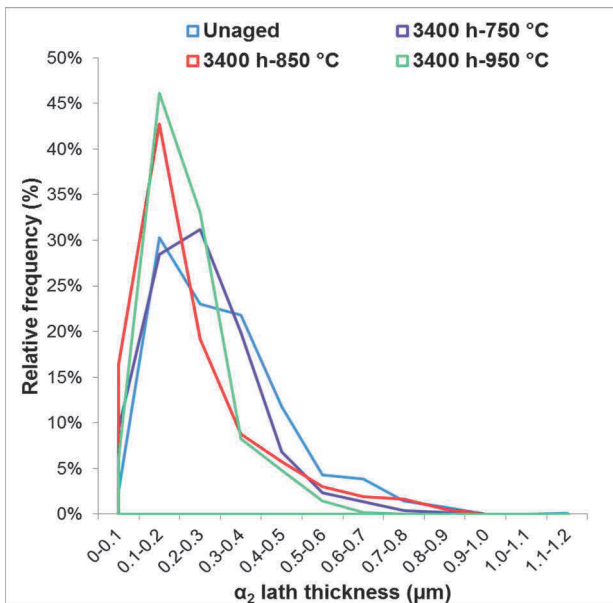


**Figure 3** The distribution of  $\alpha_2$  thickness

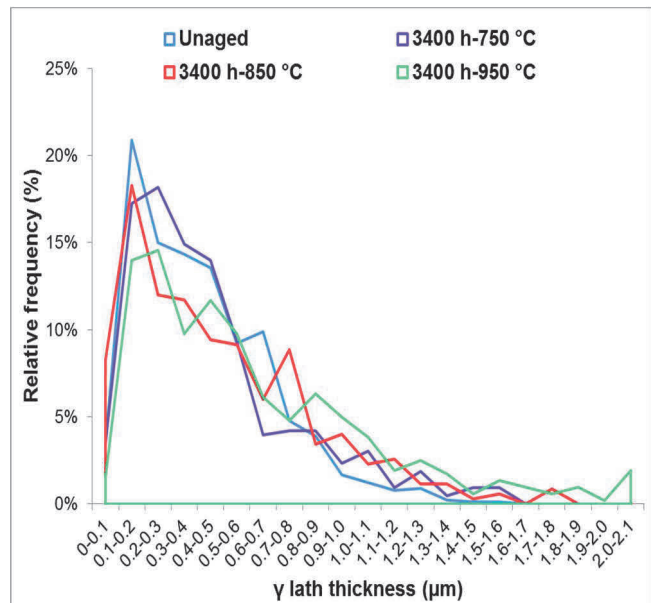


**Figure 4** The distribution of  $\gamma$  thickness

**Figure 5(a)** shows the microstructure after ageing at 850 °C for 2000 h. Several recrystallized equiaxed  $\gamma$  grains can be observed especially around the bright boride particles in lamellar grains. Recrystallized  $\gamma$  grains were seen only after exposure at 850 °C for 2000 h (not in shorter times at that temperature) and after exposure at 950 °C for 960 h or after longer periods of times and their dimensions and their frequency increased with increasing temperature and time (see **Figure 5(b)**). No recrystallized  $\gamma$  grains were observed at 750 °C even after 3400 hours. As can be seen in **Figure 5(b)** some dark precipitates were observed in recrystallized  $\gamma$  grains. A distribution of fine dark precipitates can be detected also in the lamellar  $\gamma/\alpha_2$  matrix after exposure at 850 °C for 3400 h and also at 950 °C for shorter times (first precipitates after 8 h). These precipitates are mainly formed at the lamellar interfaces and inside the  $\alpha_2$  lamellae (see **Figure 5(c)**). The XRD analysis shows occurrence of  $\text{Ti}_2\text{AlC}$  carbides in the microstructure (not shown in this article). The presence of the carbides is confirmed also the EDS analysis, which reveals an increased content of C in precipitates and the content of Ti and Al in the precipitates was approximately 2:1 indicating that these fine particles probably belong to  $\text{Ti}_2\text{AlC}$  phase. The formation of the carbides at 850, 950 °C can be explained by the dissolution of  $\alpha_2$  lamellae. The  $\alpha_2$  phase has a significantly higher solubility of carbon than the  $\gamma$  phase which leads to the precipitation of the carbides at the  $\gamma/\alpha_2$  interfaces to achieve thermodynamic equilibrium state of the alloy at the ageing temperature. **Figure 5(d)** shows the microstructure after ageing at 950 °C for 3400 h. As can be seen in this figure the dimensions and shape of  $\text{Ti}_2\text{AlC}$  precipitates show significant differences for individual grains, indicating uneven distribution of carbon. SEM observations show only very small amount of  $\text{Ti}_2\text{AlC}$  carbides after ageing at 850 °C and practically no carbides at 750 °C. However, we assume that even samples after

exposures at 750 °C contain carbides, but these carbides are not Ti<sub>2</sub>AlC (h-type) but Ti<sub>3</sub>AlC (p-type), which are characterized by smaller dimensions and their observations can mostly be made only with TEM.

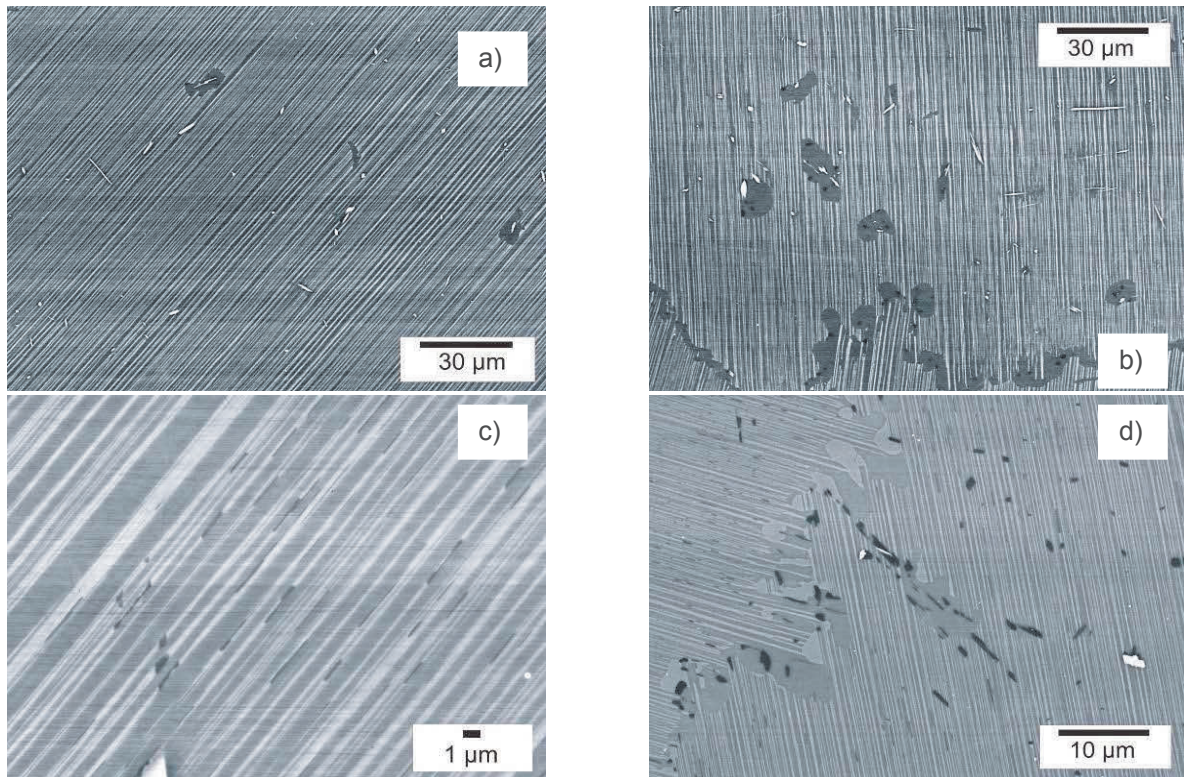


**Figure 5** SEM BSE images of lamellar structure after exposure at (a) 850 °C, 2000 h (b) 950 °C, 3400 h (c) 850 °C, 3400 h (d) 950 °C, 3400 h

### 3.3. The changes of microhardness after thermal exposure

The microhardness values obtained by measurement before exposure and after exposures at 750, 850, 950 °C for 3400 h are shown in **Table 2**. As can be seen in this table, the microhardness value decreased with increasing temperature, but the decrease was only mild 0.14, 0.17 and 0.25 GPa for 750, 850, 950 °C for 3400 h, respectively. The drop in microhardness was therefore much lower than 0.54-0.56 GPa that reported by Lapin [15] for lamellar regions in the Ti-45.2Al-2W-0.6Si-0.7B alloy after exposure at 800 °C for 3300 h. These results indicate that softening of Ti-45Al-5Nb-0.2B-0.75C is slower and cannot affect significantly the yield strength of alloy, because Vickers microhardness has a linear dependence with the yield strength for  $\gamma$ -TiAl alloys as reported previously by Lapin et al. [16]. However, roughing and growth of carbides at higher temperatures appears to be problematic, because large carbides in  $\gamma$ -TiAl reduce ductility and do not have a good effect on mechanical properties. For this reason mechanical tests in compression of the samples after the exposure will be carried out as a further activity.

**Table 2** Microhardness HV10 before and after exposure for 3400 h

Temperature (°C)	Unaged	750 °C	850 °C	950 °C
Microhardness (GPa)	4.154	4.019	3.990	3.906

## 4. CONCLUSIONS

The microstructure of fully lamellar Ti-45Al-5Nb-0.2B-0.75C (at.%) alloy is unstable during the long-term ageing at temperatures ranging from 750 to 950 °C. The dominant decomposition mode was that the  $\alpha_2$

lamellas thinned gradually and become discontinuous. Formation of recrystallized  $\gamma$  grains and  $Ti_2AlC$  carbides were also observed especially during the temperature 850 and 950 °C after prolonged heat treatment. Microhardness measurements revealed that thermal exposure caused the softening of alloy, but softening is slow and probably cannot affect significantly the yield strength.

## ACKNOWLEDGEMENTS

***This article has been elaborated in the framework of the project No. LO1203 “Regional Materials Science and Technology Centre - Feasibility Program” funded by the Ministry of Education, Youth and Sports of the Czech Republic.***

## REFERENCES

- [1] WU, X. Review of alloy and process development of TiAl alloys. *Intermetallics*, 2006, vol. 14, no. 10-11, pp. 1114-1122
- [2] APPEL, F. Microstructure and deformation of two-phase  $\gamma$ -titanium aluminides. *Materials Science and Engineering: R.*, vol. 22, no. 5, 1998, pp. 187-268.
- [3] APPEL, F. Novel design concepts for gamma-base titanium aluminide alloys. *Intermetallics*, 2000, vol. 8, no. 9-11, pp. 1283-1312.
- [4] SKOTNICOVÁ, K. Structural changes of single crystals of low-alloyed tungsten alloys at thermal cycling. *International Journal of Refractory Metals and Hard Materials*, 2012, vol. 32, pp. 61-65.
- [5] MIZUHARA, Y. Microstructure and phase stability of TiAl-W ternary alloy. *Intermetallics*, 2003, vol. 34A, no. 8, pp. 807-816.
- [6] SKOTNICOVÁ, K. Preparation and investigation of structural parameters of single crystals of low-alloyed alloys on the base of tungsten and molybdenum. *Advanced Engineering Materials*, 2013, vol. 15, No. 10, pp. 927-934.
- [7] SCHWAIGHOFER, E. Effect of carbon addition on solidification behavior, phase evolution and creep properties of an intermetallic  $\beta$ -stabilized  $\gamma$ -TiAl based alloy. *Intermetallics*, 2014, vol. 46, pp. 173-184.
- [8] PERDRIX, F. Relationships between interstitial content, microstructure and mechanical properties in fully lamellar Ti-48Al alloys, with special reference to carbon. *Intermetallics*, 2001, vol. 9, no. 9, pp. 807-815.
- [9] TIAN, W.H. Effect of carbon addition on the microstructures and mechanical properties of  $\gamma$ -TiAl alloys. *Intermetallics*, 1997, vol. 5, no. 3, pp. 237-244.
- [10] GOUMA, P. I. In situ observation of carbide and silicide precipitation in C+Si alloyed  $\gamma$ -TiAl. *Materials Letters*, 2003, vol. 57, no. 22-23, pp. 3581-3587.
- [11] JUŘICA, J. Preparation and properties of master alloys Nb-Al and Ta-Al for melting and casting of gamma-TiAl intermetallics. *Materiali in Tehnologije/Materials and Technology*, 2015, vol 49, no. 1, pp. 27-30.
- [12] ZOLLINGER, J. Influence of oxygen on solidification behaviour of cast TiAl-based alloys. *Intermetallics*, 2007, vol. 15, no. 10, pp. 1343-1350.
- [13] HECHT, U. Grain refinement by low boron additions in niobium-rich TiAl-based alloys. *Intermetallics*, 2008, vol. 16, no. 8, pp. 969-978.
- [14] KARTHIKEYAN, S. The role of microstructural stability on compression creep of fully lamellar  $\gamma$ -TiAl alloys, *Intermetallics*, 2005, vol. 13, no. 9, pp. 985-992.
- [15] LAPIN, J. Microstructural stability of a cast Ti-45.2Al-2W-0.6Si0.7B alloy at temperatures 973-1073 K, *Intermetallics*, 2006, vol. 14, no. 10 - 11, pp. 1175-1180.
- [16] LAPIN, J. Effect of  $Al_2O_3$  particles on mechanical properties of directionally solidified intermetallic Ti-46Al-2W-0.5Si alloy. *Materials Science and Engineering A*, 2003, vol. 360, no. 1-2, pp. 85-95.